



UNIVERSITY OF LEEDS

This is a repository copy of *Shakedown analysis and its application in pavement and railway engineering*.

White Rose Research Online URL for this paper:

<https://eprints.whiterose.ac.uk/176229/>

Version: Accepted Version

---

**Article:**

Wang, J and Yu, H-S [orcid.org/0000-0003-3330-1531](https://orcid.org/0000-0003-3330-1531) (2021) Shakedown analysis and its application in pavement and railway engineering. *Computers and Geotechnics*, 138. 104281. ISSN 0266-352X

<https://doi.org/10.1016/j.compgeo.2021.104281>

---

© 2021, Elsevier. This manuscript version is made available under the CC-BY-NC-ND 4.0 license <http://creativecommons.org/licenses/by-nc-nd/4.0/>.

**Reuse**

This article is distributed under the terms of the Creative Commons Attribution-NonCommercial-NoDerivs (CC BY-NC-ND) licence. This licence only allows you to download this work and share it with others as long as you credit the authors, but you can't change the article in any way or use it commercially. More information and the full terms of the licence here: <https://creativecommons.org/licenses/>

**Takedown**

If you consider content in White Rose Research Online to be in breach of UK law, please notify us by emailing [eprints@whiterose.ac.uk](mailto:eprints@whiterose.ac.uk) including the URL of the record and the reason for the withdrawal request.



[eprints@whiterose.ac.uk](mailto:eprints@whiterose.ac.uk)  
<https://eprints.whiterose.ac.uk/>

# **Shakedown analysis and its application in pavement and railway engineering**

**Dr Juan Wang<sup>1</sup>**

Email: [Juan.Wang@nottingham.edu.cn](mailto:Juan.Wang@nottingham.edu.cn)

**Professor Hai-Sui Yu<sup>2\*</sup> (FREng)**

Email: [DVC@Leeds.ac.uk](mailto:DVC@Leeds.ac.uk)

**1** Ningbo Nottingham New Materials Institute, University of Nottingham Ningbo China, 199  
Taikang East Road, Ningbo, 315100, China.

**2** School of Civil Engineering, University of Leeds, Leeds, LS2 9JT, UK.

\* Corresponding author

Acknowledgement: The Zhejiang Provincial Department of Science and Technology is acknowledged for this research under its provincial Key Laboratory Program (2020E10018).

## 1 Abstract

2 This paper has been prepared in memory of Professor Scott Sloan. It first presents a brief review of the  
3 development of shakedown analysis methods for pavement and railway engineering problems. In particular,  
4 it describes a new lower-bound method using the concept of critical residual stress fields and an upper-  
5 bound method using a nonlinear programming technique, which were developed by the authors, and then  
6 extended and applied to solve various shakedown problems in pavement and railway engineering. Moreover,  
7 this paper summarises and compares shakedown solutions for pavement and railway engineering problems,  
8 whilst highlighting the key factors that influence the shakedown limits. In addition, this paper proposes a  
9 simple, unified shakedown limit equation for pavements and railways under repeated moving surface loads.  
10 The equation includes three terms, which represent the resistances from cohesion, self-weight of the  
11 underlying soil, and self-weight of any superficial rigid layers, respectively, in a format analogous to  
12 Terzaghi's bearing capacity equation. Numerical results indicate that the coefficient in the cohesion term  
13  $N_c^{sd}$  depends on the soil friction angle; while the coefficient in the self-weight term  $N_\gamma^{sd}$  is controlled by  
14 the soil friction angle and a dimensional factor  $\gamma a/c$ . Values of  $N_c^{sd}$  and  $N_\gamma^{sd}$  for a typical rolling point  
15 contact problem are also presented and interpreted, which explain the different contribution ratios from the  
16 soil self-weight to the shakedown limits of pavement and railway problems.

17

18 **Keywords:** Shakedown; Pavement; Railway; Lower bound; Upper bound; Unified equation

## 19 1 Introduction

20 The concept of shakedown was initially proposed some 80 years ago (e.g. Bleich, 1932; Melan, 1938;  
21 Prager, 1948; Koiter, 1960). It states that when an elastic-plastic structure is subjected to a repeated or  
22 variable load and the load level is higher than yield but lower than a 'shakedown limit', the structure will  
23 gradually adapt itself to the cyclic load and respond purely elastically to the following load cycles, leading  
24 to no further exhibition of plastic strain. Otherwise, if the load level is higher than the shakedown limit, the  
25 structure will eventually fail due to alternative plasticity or excessive permanent deformation. Shakedown

26 phenomena of pavements and railways have been observed by researchers through road tests and field data  
27 analyses (e.g. Sharp and Booker, 1984; Radovsky and Murashina, 1996; Xiao et al., 2016). Many  
28 conventional cyclic triaxial tests (e.g. Lekarp and Dawson, 1998; Werkmeister et al., 2001) or cyclic hollow  
29 cylinder tests (e.g. Qian et al., 2016; Xiao et al., 2018; Wang et al., 2020a) have demonstrated the  
30 shakedown behaviours of soils, granular materials and asphalt mixtures. Moreover, by using wheel tracking  
31 tests, a series of validation experiments for shakedown theory (Juspi, 2007; Brown et al., 2008; Ravindra,  
32 2008; Ravindra and Small, 2008; Chazallon et al., 2009; Brown et al., 2012) has been carried out for single-  
33 layered or multi-layered pavement systems with different types of soils and granular materials. Very  
34 recently, Liu et al. (2020) further validated the shakedown concept for bituminous pavement structures by  
35 conducting a series of wheel tracking tests on a layered bituminous pavement structure.

36 A key task of applying shakedown concept to practical problems is to determine the shakedown limit.  
37 Compared with conventional step-by-step analysis where the full stress and strain history is required (e.g.  
38 Wang and Yu, 2013a; Liu et al., 2016; Liu et al., 2017), shakedown analysis using either static (Melan,  
39 1938) or kinematic (Koiter, 1960) shakedown theorem directly calculates the lower or upper bound of the  
40 shakedown limit thus attracts lots of attention. The application of the theoretical shakedown analysis in the  
41 design of steel rails was recognised more than 40 years ago (e.g. Doyle, 1980). Later, Sharp and Booker  
42 (1984) introduced the shakedown theory to pavement problems considering that wheels roll and slide on  
43 the surface of a cohesive-frictional material. Following that, a number of shakedown analysis methods for  
44 pavement and railway engineering problems were proposed (e.g. Ponter et al., 1985; Collins and Cliffe,  
45 1987; Raad et al., 1988; Collins and Boulbibane, 1998; Yu and Hossain, 1998; Shiau and Yu, 2000; Yu,  
46 2005; Boulbibane and Ponter, 2006; Li and Yu, 2006; Krabbenhøft et al., 2007; Nguyen et al., 2008; Zhao  
47 et al., 2008; Wang, 2011; Yu and Wang, 2012; Qian et al., 2017; Costa et al., 2018; Rahmani and Binesh,  
48 2018; Wang et al., 2018a; Wang et al., 2018b; Liu et al., 2020).

49 One objective of this paper is to provide a review of the recent development of shakedown analysis methods  
50 for pavement and railway applications, with a brief description of establishing two recent shakedown

51 analysis methods. The other objective of the paper is to summarise the key influencing factors for  
 52 shakedown limits of pavements and railways, and finally to propose a new, simple, unified equation for  
 53 shakedown limits of soils under repeated moving surface loads.

## 54 2 Shakedown theorems

55 The classical static shakedown theorem of Melan (1938) states that an elastic-perfectly plastic structure will  
 56 shakedown under repeated/cyclic loads if a time-independent self-equilibrated residual stress field can be  
 57 found, that when combined with the load-induced elastic stress field, does not violate the yield condition  
 58 anywhere in the structure. This can be expressed as:

$$59 f(\lambda \sigma_{ij}^e + \sigma_{ij}^r) \leq 0 \quad \text{Eq. 1}$$

60 where  $\sigma_{ij}^e$  is the elastic stress field induced by a unit load  $p$ ;  $\lambda$  is a dimensionless load multiplier;  $\sigma_{ij}^r$  is the  
 61 time-independent self-equilibrated residual stress field; and  $f \leq 0$  is the yield criterion for the material.

62 The classical kinematic shakedown theorem of Koiter (1960) states the structure will not shakedown under  
 63 repeated or cyclic loads if any kinematically admissible plastic strain rate cycle  $\dot{\epsilon}_{ij}^{p*}(t)$ , body force  $\mathbf{X}_i(t)$   
 64 and surface load  $\mathbf{p}_i(t)$  within prescribed limits can be found for which:

$$65 \int_0^T \left( \int_V \mathbf{X}_i \dot{\mathbf{u}}_i^* dV + \int_{S_p} \mathbf{p}_i \dot{\mathbf{u}}_i^* dS \right) dt > \int_0^T \int_V \sigma_{ij}^* \dot{\epsilon}_{ij}^{p*} dV dt \quad \text{Eq. 2}$$

66 where  $S_p$  is structure surface where external loads are specified;  $V$  is structure volume;  $T$  is time period for one  
 67 loading cycle;  $\dot{\mathbf{u}}_i^*$  and  $\sigma_{ij}^*$  are the velocity and the state of stress on the yield surface which are associated  
 68 with the kinematically admissible plastic strain rate field  $\dot{\epsilon}_{ij}^{p*}$ . Alternatively, the upper-bound shakedown  
 69 theorem can be formulated as follows when omitting the body force:

$$70 \lambda_{sd} \int_0^T \int_{S_p} \mathbf{p}_{0i} \dot{\mathbf{u}}_i^* dS dt \leq \int_0^T \int_V \sigma_{ij}^* \dot{\epsilon}_{ij}^{p*} dV dt \quad \text{Eq. 3}$$

71 where  $p_{0i}$  is a unit load,  $\lambda_{sd}$  is the shakedown load multiplier.

72 It should be noted that the two classical shakedown theorems were proved based on the assumption that the  
 73 materials satisfy Drucker's stability conditions. Therefore, they are only valid for materials obeying an  
 74 associated plastic flow rule. Nevertheless, it has been demonstrated by researchers (e.g. Maier, 1969; Pycko

75 and Maier, 1995; Boulbibane and Weichert, 1997) that the shakedown theorems can be extended to consider  
76 the materials following a non-associated flow rule if the plastic potential function  $g = 0$  is convex and  
77 contained by the yield surface.

78 Considering a rapid loading process, the dynamic shakedown concept was first introduced by Ceradini  
79 (1969). Based on additional assumptions that plastic deformations are instantaneous and the yield surface  
80 is fixed, Ceradini (1980) presented the proofs of the lower-bound and upper-bound dynamic shakedown  
81 theorems for elastic-perfectly plastic bodies subjected to a rapid loading process. The dynamic shakedown  
82 theorems take forms similar to the classical ones but use a fictitious dynamic response.

83 In general, shakedown analysis using the static or kinematic shakedown theorems obtains the shakedown  
84 limit through searching for a critical point or a critical failure mechanism. It leads to either a lower bound  
85 or an upper bound to the true shakedown limit, because the static shakedown theorem only satisfies internal  
86 equilibrium equations, yield criterion, and stress boundary conditions, while the kinematic shakedown  
87 theorem only satisfies compatibility, plastic flow rule and displacement boundary conditions.

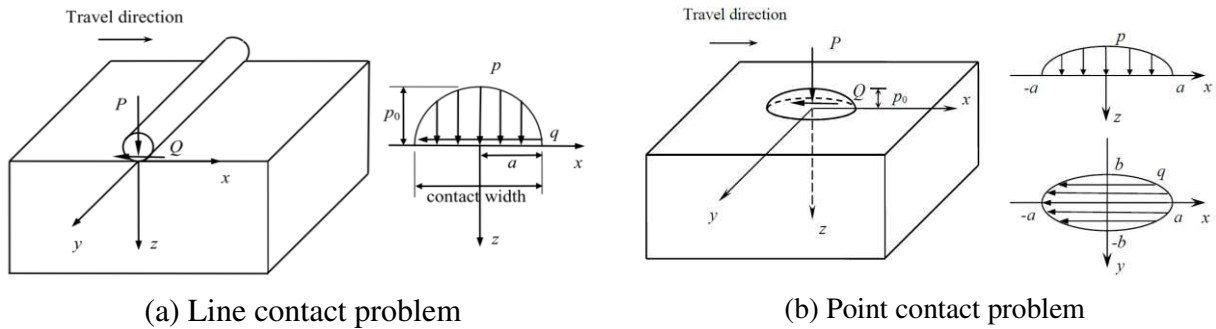
### 88 **3 Shakedown analysis methods for pavements and railways**

#### 89 3.1 Simplification of problems

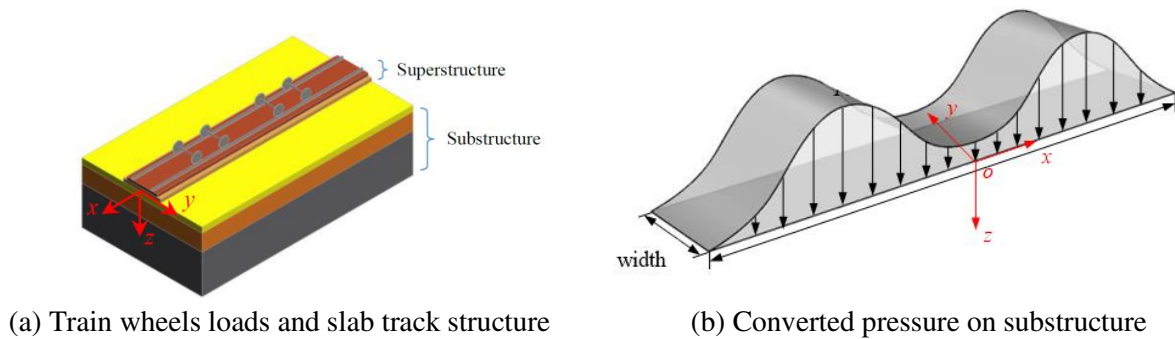
90 Shakedown of an elastic-plastic half space subjected to rolling and sliding contact is fundamental to the  
91 analyses of pavement and railway engineering problems. Two basic rolling and sliding contact problems  
92 are line and point contacts. The line contact problem assumes a simple situation in which the load is applied  
93 over a certain contact width by a long roller, whilst the point contact problem considers a surface contact  
94 loading limited to a circular, an elliptical, or a rectangular contact area. If the normal load is denoted as  $P$ ,  
95 its tangential counterpart  $Q$  can be expressed as  $\mu P$ , where  $\mu$  is a frictional coefficient. It is usually assumed  
96 that the normal and shear stresses over the contact area are correlated by the frictional coefficient, and they  
97 distributed in a Hertz, Trapezoid or uniform shape. For instance, using the Hertz formulation, the  
98 distributions of normal and shear stresses are depicted in Figure 1, in which the  $x$ -axis is the travel direction.

99 The Hertz load distribution has a maximum compressive pressure at the center  $p_0 = 2P/\pi a$  for the line  
 100 contact problem, and  $p_0 = 3P/2\pi ab$  for the point contact problem.

101 For railway problems and some pavement situations, the stresses due to neighbouring wheels overlap within  
 102 some regions in the ground. Therefore, shakedown analysis needs to be conducted considering that several  
 103 wheel loads move simultaneously on the surface (e.g. Collins et al., 1993a; Wang et al., 2018a). Furthermore,  
 104 the analysis of railway problems needs to take the effect of superstructure components into account. This  
 105 can be done by converting a set of neighbouring train wheel loads as well as the influence of the  
 106 superstructure into a distributed pressure on the top of the substructure (e.g. Liu et al., 2018; Wang et al.,  
 107 2018a; Wang et al., 2020b), as shown in Figure 2.



108  
 109 Figure 1: Rolling and sliding contact problems



111  
 112 Figure 2: Conversion of train loads into a pressure

## 113 3.2 Static shakedown analysis methods

### 114 3.2.1 *Recent development*

115 Over a number of years, shakedown analysis methods based on the static shakedown theorem were  
116 developed for the line contact problem (e.g. Sharp and Booker, 1984; Sharp, 1985; Raad et al., 1988; Raad  
117 et al., 1989a, 1989b; Raad and Weichert, 1995; Radovsky and Murashina, 1996; Yu and Hossain, 1998;  
118 Boulbibane et al., 2000; Shiau and Yu, 2000; Krabbenhøft et al., 2007; Nguyen, 2007; Nguyen et al., 2008;  
119 Zhao et al., 2008). Because of the two-dimensional nature of the line contact problem, the solutions can  
120 only be considered as approximate ones. In recent years, efforts have been devoted to develop shakedown  
121 analysis methods considering more realistic loading situations in pavement and railway engineering. Based  
122 on the consideration, the problem becomes three-dimensional, and therefore it is much more difficult to  
123 derive relevant shakedown solutions. Shiau (2001) extended the linear programming technique of Yu and  
124 Hossain (1998) to solve the three-dimensional pavement shakedown problem. Although some reasonable  
125 results were obtained, it was found that the size of the linear programming problem became prohibitively  
126 large when a finer mesh was applied in the three-dimensional case. Nguyen et al. (2008) utilised an interior-  
127 point method to solve pavement shakedown problems considering a rounded Mohr-Coulomb or a von Mises  
128 yield criterion. Both two-dimensional and three-dimensional rolling and sliding contact problems were  
129 analysed, but the numerical results for the three-dimensional case cannot be yet considered reliable.

130 To efficiently solve the three-dimensional problem, Yu (2005) obtained an analytical necessary condition  
131 for shakedown limits of a cohesive-frictional half-space under a moving point load. Wang (2011) and Yu  
132 and Wang (2012) developed a rigorous lower-bound shakedown analysis method by deriving two critical  
133 residual stress fields, and thus reducing the problem to a simple mathematical optimisation problem. The  
134 analytical solutions of elastic stresses in a half-space under an elliptical Hertz load was used, so that the  
135 results can be used to benchmark numerical shakedown limits. The critical residual stress fields obtained in  
136 this method were also found in agreement with the numerical results obtained through a step-by-step finite  
137 element analysis and a mesh-free method for both line contact and point contact problems (Wang and Yu,



138 2013a; Liu et al., 2018; Rahmani and Binesh, 2018). Considering the cross-anisotropic behaviour of soils  
139 and pavement materials, Wang and Yu (2014) developed a shakedown analysis method to allow the  
140 variation of elastic and plastic material properties with direction.

141 Based on the lower-bound shakedown analysis method of Yu and Wang (2012), a number of extensions  
142 and applications for pavement and railway problems were conducted. In the field of pavement engineering,  
143 the method was utilised to solve pavement design problems (Wang and Yu, 2013b) and to compare with  
144 the analytical design approach in the UK for flexible road pavements (Wang et al., 2016). Liu et al. (2016)  
145 extended the method to examine the influence of dilation angle on lower-bound shakedown limits of  
146 pavements. By introducing a numerical approach which calculates the traffic-induced dynamic elastic stress  
147 field, Qian et al. (2017) studied the influence of traffic speed on shakedown limits, and the work was further  
148 extended to consider the effects of cross-anisotropic materials (Qian et al., 2018) and frictional coefficient  
149 (Qian et al., 2020). Since the properties of asphalt mixtures are highly dependent on temperature, Liu et al.  
150 (2020) proposed a temperature-dependent shakedown approach to obtain shakedown limits of asphalt  
151 pavements. In the field of railway engineering, although the shakedown solutions of steel rails have been  
152 studied for many years (e.g. Doyle, 1980; Bower and Johnson, 1991; Kapoor and Williams, 1994; Dyson  
153 et al., 1999; Ringsberga et al., 2005; Hasan, 2019), it was not until very recently that the shakedown analysis  
154 method of Yu and Wang (2012) was extended to allow the calculation of shakedown solutions for railway  
155 structures. Considering a typical slab track for high-speed railways, Wang et al. (2018a) investigated the  
156 dynamic shakedown limits of slab track substructures and revealed the relation between the dynamic  
157 shakedown limits and critical speeds. Liu et al. (2018) focused on the influence of a depth-dependent  
158 stiffness modulus on shakedown limits. Costa et al. (2018) considered at-rest stresses in the ground and  
159 adopted a 2.5D approach to calculate dynamic elastic stresses; and therefore the influences of train geometry,  
160 track stiffness, and soil improvement were examined for a slab track system. There were also some efforts  
161 in applying the shakedown analysis method of Yu and Wang (2012) in determining the shakedown limits  
162 of ballasted railways (e.g. Zhuang et al., 2019); however their analyses did not consider the spaced sleepers

163 thus violated one basic assumption of the rolling and sliding contact problems that the residual stresses  
 164 should be independent of the travel direction.

### 165 3.2.2 Static shakedown analysis based on critical residual stress fields

166 According to Yu and Wang (2012), for the three-dimensional rolling and sliding contact problems,  
 167 symmetry and other considerations impose some constraints on the residual stresses: (1) the residual stresses  
 168 must be independent of  $x$ ; (2)  $\sigma_{zz}^r$  and  $\sigma_{xz}^r$  must be zero; (3) the residual stress itself must satisfy the yield  
 169 condition, i.e.,  $f(\lambda\sigma_{ij}^r) \leq 0$ . A detailed analysis of the possible residual stresses can be found in Yu and  
 170 Wang (2012) and Yu (2005). The validity of the residual stresses has also been verified in the numerical  
 171 studies of Shiau (2001) and Liu et al. (2017). Assuming that the material is described by the Mohr-Coulomb  
 172 model and the critical planes are  $x$ - $z$  planes, the static shakedown theorem (Eq. 1) can be rewritten as follows:

$$173 \quad f = (\sigma_{xx}^r + M)^2 + N \leq 0 \quad \text{Eq. 4}$$

174 where  $\sigma_{xx}^r$  is time-independent and self-equilibrated;  $M = \lambda\sigma_{xx}^e - \lambda\sigma_{zz}^e + 2 \tan \phi (c - \lambda\sigma_{zz}^e \tan \phi)$ ;  $N =$   
 175  $4(1 + \tan^2 \phi)[(\lambda\sigma_{xx}^e)^2 - (c - \lambda\sigma_{zz}^e \tan \phi)^2]$ ;  $c$  and  $\phi$  are cohesion and friction angle of the material,  
 176 respectively.

177 Based on the conditions for residual stresses and the shakedown condition Eq. 4, Yu and Wang (2012)  
 178 found that the actual residual stress field must lie within a region determined by two critical stress fields  
 179  $\sigma_{xx-l}^r$  (denoted as ‘maximum smaller root’) and  $\sigma_{xx-u}^r$  (denoted as ‘minimum larger root’):

$$180 \quad \sigma_{xx-l}^r = \max_{z=j}^{-\infty \leq x \leq \infty} (-M_i - \sqrt{-N_i}) \quad \text{Eq. 5}$$

$$181 \quad \sigma_{xx-u}^r = \min_{z=j}^{-\infty \leq x \leq \infty} (-M_i + \sqrt{-N_i}) \quad \text{Eq. 6}$$

182 where  $i$  represents a point in the half-space; and  $j$  represents a depth. When the applied load is at the  
 183 shakedown limit, the actual residual stress at a depth  $z = j$  must be no smaller than  $\sigma_{xx-l}^r$  and no higher  
 184 than  $\sigma_{xx-u}^r$ , and the critical point of the half-space is located at the depth where the two critical residual  
 185 stresses just intersect.

186 By substituting Eq. 5 or Eq. 6 into Eq. 4, the shakedown problem can be expressed as the following  
187 mathematical formulation:

$$\begin{aligned} \lambda_{sd} &= \max(\lambda) \\ \text{s. b. } &\begin{cases} f(\sigma_{xx}^r(\lambda\sigma^e), \lambda\sigma^e) \leq 0 \text{ for all points} \\ \sigma_{xx}^r(\lambda\sigma^e) = \sigma_{xx-l}^r \text{ or } \sigma_{xx-u}^r \end{cases} \end{aligned} \quad \text{Eq. 7}$$

189 Since the elastic stress fields  $\sigma^e$  and the critical residual stress fields all depend on the load multiplier  $\lambda$ ,  
190 Eq. 7 can be easily solved by using the procedure suggested in Wang (2011) and Yu and Wang (2012).

### 191 3.3 Kinematic shakedown analysis methods

#### 192 3.3.1 *Recent development*

193 Based on Koiter's kinematic shakedown theorem, Ponter et al. (1985) obtained shakedown limits of a  
194 cohesive half-space under a point contact loading. Two distinct failure modes were considered in the  
195 analysis: incremental collapse and alternating plasticity. Considering that the rate of plastic working per  
196 unit length on the slip line is the product of cohesion with the tangential velocity jump, Collins and Cliffe  
197 (1987) presented upper-bound shakedown solutions of a cohesive-frictional half-space under a moving two-  
198 dimensional or three-dimensional surface load. This method was extended to two-layered pavements by  
199 using a different shape of the slip channel (Collins et al., 1993a; Collins et al., 1993b), and then it was  
200 improved by introducing rut failure mechanisms (Collins and Boulbibane, 1998, 2000; Boulbibane et al.,  
201 2005).

202 Recently, the linear matching method, originally proposed for limit and shakedown analyses of metal  
203 structures under static or cyclic load (e.g. Ponter and Carter, 1997; Ponter and Engelhardt, 2000; Chen and  
204 Ponter, 2005; Ponter et al., 2006), has been applied to the pavement shakedown problem (Boulbibane and  
205 Ponter, 2005, 2006). The basic idea of this method is that the stress and strain fields for the nonlinear  
206 material behaviours may be simulated by the solution of linear problems where linear moduli vary with  
207 time and space. Li and Yu (2006) proposed a nonlinear programming approach for kinematic shakedown  
208 analysis of cohesive-frictional materials. It was further extended to consider a general yield condition with  
209 a non-associated plastic flow rule (Li, 2009). The approach has been applied to solve pavement shakedown

210 problems with materials following an associated or a non-associated plastic flow rule. The approach of Li  
 211 and Yu (2006) will be briefly explained in the following subsection. Apart from that, the work of Ponter et  
 212 al. (1985) could also be very useful in terms of understanding the kinematic shakedown analysis.

### 213 3.3.2 Kinematic shakedown analysis using a nonlinear programming approach

214 By applying the principle of virtual work, the kinematic shakedown theorem Eq. 3 can be written as:

$$215 \lambda_{sd} \int_0^T \int_V \boldsymbol{\sigma}_{ij}^e \dot{\boldsymbol{\epsilon}}_{ij}^{p*} dV dt \leq \int_0^T \int_V \boldsymbol{\sigma}_{ij}^* \dot{\boldsymbol{\epsilon}}_{ij}^{p*} dV dt \quad \text{Eq. 8}$$

216 in which  $\boldsymbol{\sigma}_{ij}^e$  is the linear elastic stress response to external actions. Eq. 8 can be re-expressed as the

217 following problem using the mathematical programming theory (Li and Yu, 2006):

$$218 \lambda_{sd} = \min_{\boldsymbol{\epsilon}_{ij}^p, \Delta \mathbf{u}} \int_0^T \int_V \boldsymbol{\sigma}_{ij}^* \dot{\boldsymbol{\epsilon}}_{ij}^{p*} dV dt$$

$$\text{s. b.} \begin{cases} \int_0^T \int_V \boldsymbol{\sigma}_{ij}^e \dot{\boldsymbol{\epsilon}}_{ij}^{p*} dV dt = 1 \\ \Delta \boldsymbol{\epsilon}_{ij}^p = \int_0^T \dot{\boldsymbol{\epsilon}}_{ij}^{p*} dt = \frac{1}{2} (\Delta \mathbf{u}_{i,j} + \Delta \mathbf{u}_{j,i}) & \text{in } V \\ \Delta \mathbf{u}_i = \int_0^T \dot{\mathbf{u}}_i dt & \text{in } V \\ \Delta \mathbf{u}_i = 0 & \text{on } S_u \end{cases} \quad \text{Eq. 9}$$

219 in which  $\Delta \boldsymbol{\epsilon}_{ij}^p$  and  $\Delta \mathbf{u}_i$  are cumulative plastic strain and displacement fields at the end of one loading cycle

220 over one time cycle  $[0, T]$ , respectively; and  $S_u$  is displacement boundary.

221 Many widely used yield criteria for cohesive-frictional materials can be expressed as:

$$222 F(\boldsymbol{\sigma}) = \boldsymbol{\sigma}^T \mathbf{P} \boldsymbol{\sigma} + \boldsymbol{\sigma}^T \mathbf{Q} - 1 = 0 \quad \text{Eq. 10}$$

223 in which  $\boldsymbol{\sigma}$  is the stress vector;  $F(\boldsymbol{\sigma})$  defines a yield function in terms of strength parameter;  $\mathbf{P}$  and  $\mathbf{Q}$  are

224 coefficient matrices and vector which are related to strength properties of the material.

225 By using the general yield equation and a specific plastic flow rule, the plastic strain rate field can be

226 obtained. For the case with an associated plastic flow rule, it can be written as:

$$227 \dot{\boldsymbol{\epsilon}}^p = 2\dot{\eta} \mathbf{P} \boldsymbol{\sigma} + \dot{\eta} \mathbf{Q} \quad \text{Eq. 11}$$

$$228 \text{ where } \dot{\eta} = \sqrt{\frac{(\dot{\boldsymbol{\epsilon}}^p)^T \mathbf{P}^{-1} \dot{\boldsymbol{\epsilon}}^p}{4 + \mathbf{Q}^T \mathbf{P}^{-1} \mathbf{Q}}}.$$

229 Then the plastic dissipation power can be obtained as follows:

$$230 \quad \sigma_{ij}^e \dot{\epsilon}_{ij}^{p*} = \frac{1}{2\dot{\eta}} (\dot{\epsilon}^p)^T \mathbf{P}^{-1} \dot{\epsilon}^p - \frac{1}{2} (\mathbf{Q})^T \mathbf{P}^{-1} \dot{\epsilon}^p \quad \text{Eq. 12}$$

231 Following the technique of König (1987), it is assumed that if a structure reaches a state of shakedown  
 232 under any load vertices, it will shake down under the whole load domain. The admissible plastic strain  
 233 cycles on the vertices  $\mathbf{P}_k$  ( $k = 1, 2, \dots, l$ ) can generate plastic strain increment:

$$234 \quad \boldsymbol{\epsilon}_k^{p*} = \int_{\tau_k} \dot{\boldsymbol{\epsilon}}^{p*} dt \quad \text{Eq. 13}$$

235 The cumulative plastic strain at the end of one loading cycle can be calculated from:

$$236 \quad \Delta \boldsymbol{\epsilon}^{p*} = \sum_{k=1}^l \boldsymbol{\epsilon}_k^{p*} \quad \text{Eq. 14}$$

237 By substituting Eq. 12 and Eq. 14 into Eq. 9, the shakedown analysis becomes an optimisation problem  
 238 with several equality constrains (Eq. 15) which can be solved according to the technique in Li and Yu  
 239 (2006).

$$240 \quad \lambda_{sd} = \min_{\substack{\boldsymbol{\epsilon}_k^{p*}, \Delta \mathbf{u}}} \sum_{k=1}^l \int_V \left( \frac{1}{2\dot{\eta}} (\boldsymbol{\epsilon}_k^{p*})^T \mathbf{P}^{-1} \boldsymbol{\epsilon}_k^{p*} - \frac{1}{2} (\mathbf{Q})^T \mathbf{P}^{-1} \boldsymbol{\epsilon}_k^{p*} \right) dV$$

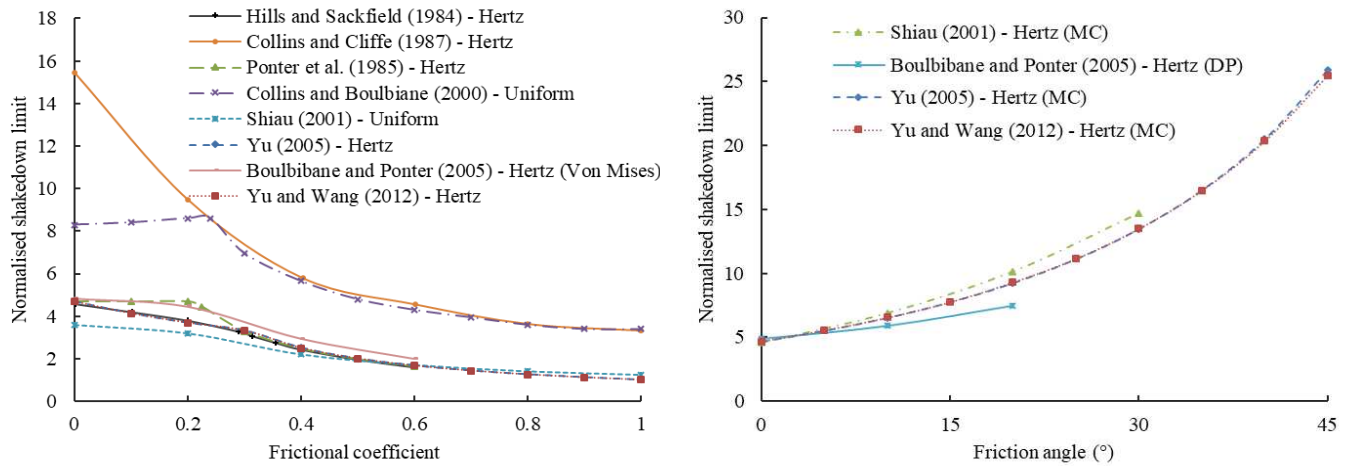
$$\text{s. b. } \begin{cases} \sum_{k=1}^l \int_V (\sigma_k^e)^T \boldsymbol{\epsilon}_k^{p*} dV = 1 \\ \Delta \boldsymbol{\epsilon}_{ij}^p = \sum_{k=1}^l \boldsymbol{\epsilon}_k^{p*} = \frac{1}{2} (\Delta \mathbf{u}_{i,j} + \Delta \mathbf{u}_{j,i}) & \text{in } V \\ \Delta u_i = 0 & \text{on } S_u \end{cases} \quad \text{Eq. 15}$$

## 241 4 Shakedown solutions for pavement problems

### 242 4.1 Effects of cohesion, friction angle, and frictional coefficient

243 Three-dimensional shakedown analysis of pavements usually assumes that the contact loading is limited  
 244 within a circle of radius  $a$ . It was found the shakedown limit is always proportional to the material cohesion  
 245  $c$  when omitting material self-weight. Hence, the shakedown solution is normally represented by a  
 246 normalised shakedown limit  $\lambda_{sd} p/c$ . Figure 3 exhibits a comparison of existing lower bound shakedown  
 247 solutions (Hills and Sackfield, 1984; Shiau, 2001; Yu, 2005; Yu and Wang, 2012) and upper bound  
 248 shakedown solutions (Ponter et al., 1985; Collins and Cliffe, 1987; Collins and Boulbibane, 2000;  
 249 Boulbibane and Ponter, 2005) for such a three-dimensional situation. For the case with cohesive materials,  
 250 the upper-bound shakedown limits are usually higher than the lower-bound shakedown limits. The upper-

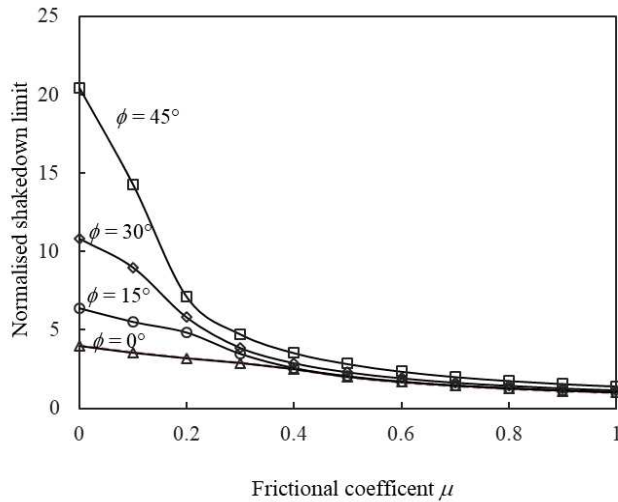
251 bound solutions of Ponter et al. (1985) agree well with the lower-bound solutions for cases  $\mu = 0$  and  $\mu \geq$   
 252 0.3, which implies true shakedown limits. The static shakedown limit always decreases with increasing  
 253 frictional coefficient, whereas the kinematic shakedown limit barely changes between  $\mu = 0$  and  $\mu = 0.2$ .  
 254 As for cohesive-frictional materials, it is clear that the static and kinematic shakedown limits are raised by  
 255 increasing friction angle. The lower-bound shakedown solutions for Mohr-Coulomb materials are close,  
 256 and they are slightly higher than Boulbibane and Ponter (2005)'s kinematic solutions, because an  
 257 incompressible non-associated flow and a Drucker-Prager material was used instead. Figure 4 demonstrates  
 258 and compares the interactive effect of friction angle and frictional coefficient on the normalised lower-  
 259 bound shakedown limits for both line contact and point contact problems (Wang, 2011). When the frictional  
 260 coefficient is relatively small, the critical point is located at a depth below the pavement surface; otherwise,  
 261 failure initiates at the surface.



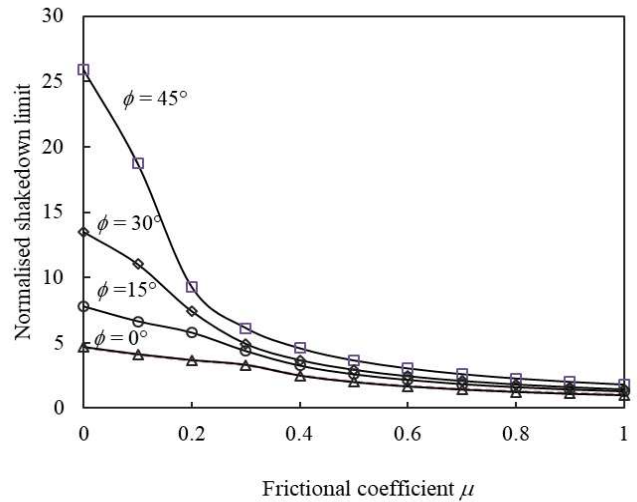
(a) Cohesive material

(b) Cohesive-frictional material,  $\mu = 0$

Figure 3: Comparison of shakedown limits for a point contact problem



(a) Line contact problem



(b) Point contact problem

Figure 4: Comparison of static shakedown limits for line and point contact problems

264

265

266 4.2 Effect of elongated contact area

267 For the cases with an elliptical contact area, if the area of the contact loading does not change, a reduction  
 268 of the aspect ratio  $b/a$  (refers to Figure 1b) leads to a rise of the normalised shakedown limit; meanwhile,  
 269 the critical point tends to move towards the surface (Yu and Wang, 2012).

270 4.3 Effect of stiffness ratio

271 In flexible pavements, upper layers normally have higher values of stiffness modulus than lower layers. If  
 272 a quasi-static situation is considered, the normalised shakedown limit is affected by the stiffness ratios rather  
 273 than the absolute values of the stiffness modulus. Moreover, there always exists an optimum stiffness ratio  
 274 that provides the maximum resistance (i.e. highest shakedown limit), which represents the movement of the  
 275 critical point from one layer to another (Sharp and Booker, 1984; Shiau, 2001; Wang and Yu, 2013b).

276 4.4 Effect of layer thickness

277 Increasing the thickness of an upper layer usually raises shakedown limit; however, when the thickness  
 278 exceeds a certain value, the shakedown limit barely changes with the layer thickness or the stiffness ratio.  
 279 This is because the failure is totally controlled by the strength properties of the upper layer (Shiau and Yu,  
 280 2000; Boulbibane et al., 2005; Wang and Yu, 2013b); and the corresponding layer thickness can be  
 281 considered as the depth of influence of the contact loading.

#### 282 4.5 Effect of anisotropy

283 For cases with cross-anisotropic materials, the elastic parameters which mainly affect shakedown limits are  
284 stiffness modulus ratio  $E_v/E_h$  and shear modulus ratio  $G_{vh}/G_h$  (the subscripts  $v, h$  represent vertical and  
285 horizontal directions, respectively). When the material surface is critical, the shakedown limit mainly  
286 depends on the shear modulus ratio; otherwise, it is dominated by the stiffness modulus ratio (Wang and  
287 Yu, 2014).

288 For the plastic part, it is normally assumed that cohesion of the material changes with the direction. With  
289 rising cohesion ratio  $c_v/c_h$ , the normalised shakedown limit  $\lambda P/c_h$  increases until a maximum value is  
290 reached, which is controlled by the subsurface failure mode. For any cases with  $c_v/c_h > 1$ , Wang and Yu  
291 (2014) found that a peak shakedown limit exists at a frictional coefficient  $\mu > 0$ . This is different from  
292 isotropic solutions which are always largest at  $\mu = 0$  (i.e. normal loading only).

#### 293 4.6 Effect of plastic flow rule

294 For cohesive-frictional materials, a dilation angle  $\psi$  ( $0 \leq \psi < \phi$ ) is often used to describe the plastic  
295 potential. Both upper-bound (Li and Yu, 2006) and lower-bound (Liu et al., 2016) solutions suggested that  
296 the pavement shakedown limits are reduced due to the decrease of the dilation angle.

#### 297 4.7 Effect of temperature

298 At a higher temperature, stiffness moduli and cohesions of asphalt mixtures are lower; consequently, the  
299 shakedown limit of each pavement layer is reduced, especially for the asphaltic layer (Liu et al., 2020).  
300 The shakedown approach is most applicable for asphalt mixtures in which the aggregate skeleton takes  
301 most of the stresses.

### 302 **5 Shakedown solutions for railway problems**

303 Shakedown analysis of railway problems is more complex than pavement problems since it requires a  
304 careful consideration and analysis of the superstructure. Take a typical Rheda 2000 single track system as  
305 an example (Figure 2), its superstructure includes rails, pads, fastening systems, slab, and concrete base;  
306 while its substructure contains an anti-frozen layer, a prepared subgrade, and subsoil. In railway problems,



307 the sleepers are spaced at a certain interval, so that the residual stresses should be periodic along the travel  
308 direction, especially in the region close to the sleepers. Despite of that, for typical slab tracks, the stresses  
309 at or below the surface of the substructure has become independent of the locations of the sleepers due to  
310 high rigidity of the slab and the concrete base. Based on this fact, shakedown analysis was performed on  
311 slab track substructures (Liu et al., 2018; Wang et al., 2018a; Liu and Wang, 2019). It was considered that  
312 the superstructure components act together as a single infinite Euler-Bernoulli beam, while the supporting  
313 substructure behaves as a Winkler's foundation, so that the axle loads and the superstructure can be  
314 converted into a moving pressure directly acting on the top of the substructure, as shown in Figure 2.  
315 Alternatively, shakedown analysis of slab tracks can be carried out by directly modelling a track-ground  
316 system (Costa et al., 2018). In this section, several additional factors that greatly affect the shakedown limits  
317 of railways will be discussed.

#### 318 5.1 Effect of at-rest stress

319 In railway problems, the load-influenced depth is much greater than that in pavements. For instance, an  
320 influencing depth of 7m was obtained in Tang et al. (2015) for a typical railway structure. Therefore, the  
321 effect of at-rest stress cannot be neglected in the shakedown analysis of railways. It was noted by Costa et  
322 al. (2018) that the shakedown limit could be underestimated if the at-rest stresses were not taken into  
323 account. Despite of that, it is still unclear of the contribution proportion of the self-weight on the shakedown  
324 limit.

#### 325 5.2 Effect of depth-dependent stiffness

326 One typical feature of the clayey subsoil is that its stiffness increases with depth. Liu et al. (2018) found an  
327 increment of stiffness could have two effects on the shakedown limit. First, the pressure distribution on the  
328 substructure becomes relatively uneven, leading to higher stresses close to the surface thus a smaller  
329 shakedown limit of the surface layer. Second, the layer stiffness ratios are changed, causing more stresses  
330 transferred to the subsoil thus a smaller shakedown limit of the subsoil.

331 5.3 Effect of train speed

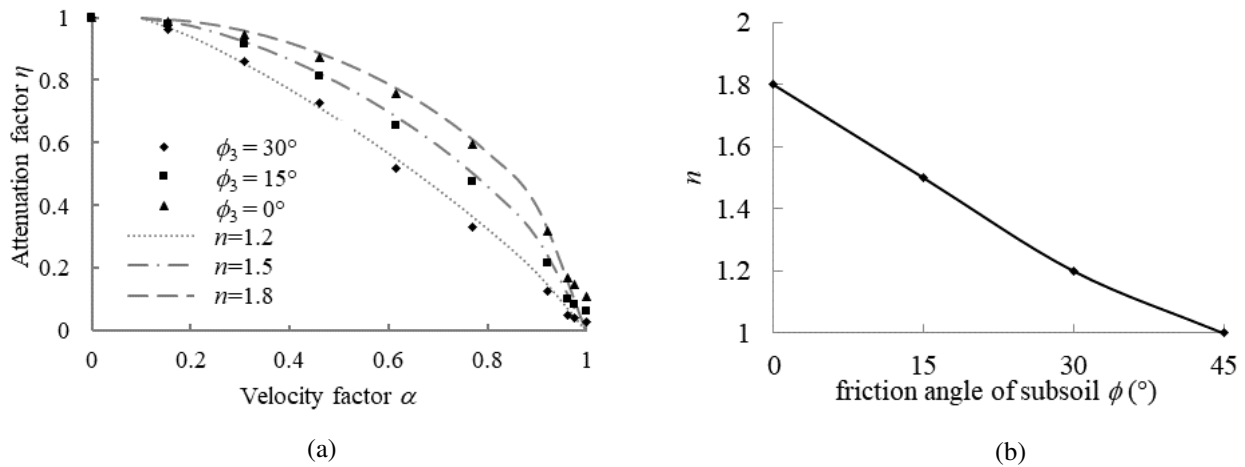
332 Train speed is critical in the design of high-speed railways. Wang et al. (2018a) revealed the dynamic  
 333 shakedown limit of a slab track substructure depends on a velocity factor  $\alpha = V/V_{cr}$  ( $V$  is train velocity;  
 334  $V_{cr}$  is the critical velocity) rather than the absolute value of train velocity. An attenuation factor  $\eta$  was  
 335 introduced to relate the dynamic shakedown limit  $\lambda_{sd}^d P$  with the static shakedown limit  $\lambda_{sd}^s P$ :

336 
$$\lambda_{sd}^d P = \eta \lambda_{sd}^s P \tag{Eq. 16}$$

337 With increasing velocity factor, the change of the shakedown limit from the static solution also depends on  
 338 the friction angle of subsoil  $\phi_3$  (Figure 5a); however, it was barely affected by the layers above the subsoil  
 339 (Wang et al., 2021). Therefore, a fitting equation is proposed:

340 
$$\eta = \begin{cases} 1 & \text{for } \alpha \leq 0.1 \\ (1 - \eta_{cr}) \times \sqrt[n]{1 - \left(\frac{\alpha - 0.1}{0.9}\right)^n} + \eta_{cr} & \text{for } 0.1 < \alpha \leq 1 \end{cases} \tag{Eq. 17}$$

341 where  $n$  is a coefficient depending on the friction angle of subsoil, the value of which can be obtained from  
 342 Figure 5b;  $\eta_{cr}$  is the attenuation factor at the critical velocity, the value of which can be taken as 0 in most  
 343 design situations (exception occurs when the stiffness of subsoil is extremely low compared to the stiffness  
 344 of the upper layers).



345  
 346 Figure 5: Influences of velocity factor and friction angle of subsoil on attenuation factor

## 347 **6 A unified shakedown limit equation for rolling and sliding problems**

348 As reviewed in the previous two sections, many studies have been devoted to obtain shakedown limits for  
349 pavements and railways, and to analyse the influences of various factors. Many of the studies were dedicated  
350 to very specific cases and there have been no general equations that would consider various contributing  
351 factors. It should be noted that although the shakedown solutions vary significantly for different problems,  
352 they share some common trends and key factors. In this section, a simple, unified equation for the  
353 shakedown limits of cohesive-frictional materials under repeated moving surface loads is proposed, which  
354 is applicable to both pavement and railway problems. This equation aims to bring together the effects of  
355 several basic and key factors.

### 356 **6.1 A unified shakedown limit equation**

357 Fundamentally, the shakedown limit is the bearing capacity of the material under the action of a repeated  
358 moving surface load. A natural choice of the format of the unified equation would be the one that is similar  
359 to the classical Terzaghi's bearing capacity equation (Eq. 18).

$$360 \quad q_{ult} = N_c c + N_q q_0 + N_\gamma \gamma a \quad \text{Eq. 18}$$

361 where  $N_c$ ,  $N_q$ , and  $N_\gamma$  give the resistances due to the material cohesion  $c$ , the overburden stress  $q_0$ , and the  
362 self-weight of the material, respectively;  $\gamma$  is the unit weight of the soil; and  $a$  is a half width of the contact  
363 area considering a strip footing. This equation is basic, concise and powerful, each term of which has a clear  
364 physical meaning. For pavements and railways under moving surface loads, the shakedown limit of the  
365 rolling and sliding contact problem (or called 'cyclic capacity'), can be expressed in an analogous format:

$$366 \quad q_{ult}^{sd} = N_c^{sd} c + N_q^{sd} q_0 + N_\gamma^{sd} \gamma a \quad \text{Eq. 19}$$

367 where  $N_c^{sd}$  and  $N_\gamma^{sd}$  stand for the resistances from the cohesion and the self-weight of the underlying  
368 material, respectively;  $N_q^{sd}$  represents the resistance from overburden stress due to the self-weight of the  
369 structural components above the cohesive-frictional materials. Notice that the overburden term only applies  
370 if there exists one or more layers of rigid materials on the top of the cohesive-frictional materials, such as

371 slabs and concrete base on the top of the substructure in a slab track, or a concrete layer above a granular  
372 layer in a pavement structure.

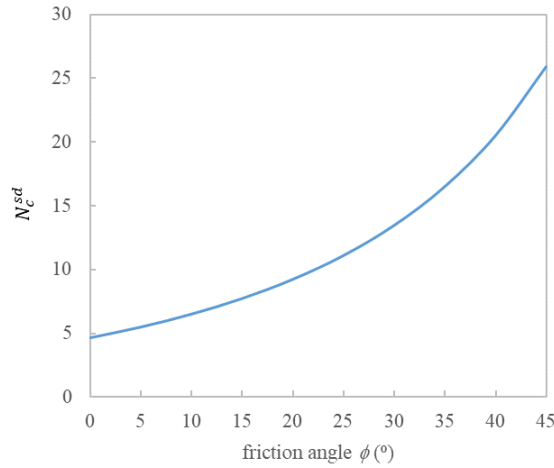
373 Similar to Terzaghi's bearing capacity equation, by including a set of correction coefficients in the  
374 expression, Eq. 19 can also be extended to consider the effects of other factors, such as the shape of the  
375 contact area, the distribution of the pressure, the horizontal component of the load, anisotropic soil and so  
376 on. Consequently, it can be readily used to estimate the shakedown limit (or cyclic capacity) of various  
377 pavements and railways under traffic loads.

## 378 6.2 $N_c^{sd}$ and $N_\gamma^{sd}$ for a rolling point contact problem

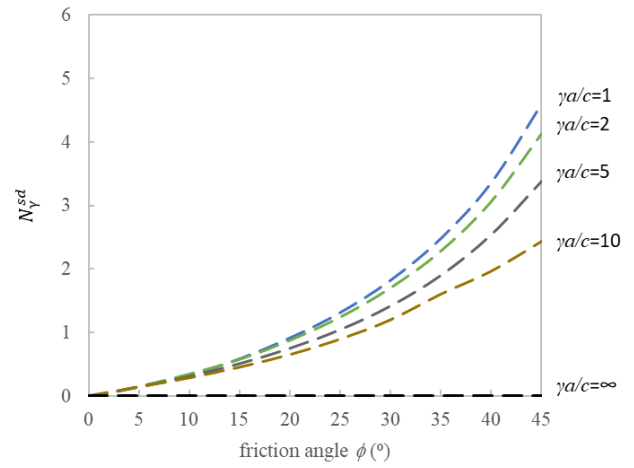
379 For one basic rolling point contact problem in which a homogenous and isotropic half-space is subjected to  
380 a moving Hertz contact loading limited within a circle of radius  $a$ , the values of the coefficients  $N_c^{sd}$  and  
381  $N_\gamma^{sd}$  are presented in Figure 6 as examples. Those coefficients were calculated based on the lower-bound  
382 shakedown analysis method of Yu and Wang (2012).  $N_c^{sd}$  is a function of the material friction angle  $\phi$ . It  
383 is obtained by applying zero self-weight in the calculation of the shakedown solutions.  $N_\gamma^{sd}$  is a function of  
384 the friction angle  $\phi$  and a dimensionless factor  $\gamma a/c$ . It is obtained by deducting the contribution of  
385 cohesion from the obtained shakedown limit, as follows:

$$386 \quad N_\gamma^{sd} = (q_{ult}^{sd} - N_c^{sd} c) / \gamma a \quad \text{Eq. 20}$$

387 As can be seen,  $N_\gamma^{sd}$  is only one fifth of  $N_c^{sd}$  at its maximum. Since typical asphalt mixtures have high  
388 values of cohesion, say 200~1000kPa (Liu et al, 2020), the contribution of the self-weight term will be very  
389 small compared to the cohesion term. This explains why the shakedown limits of asphalt pavements are  
390 barely affected by the self-weight.



(a)  $N_c^{sd}$



(b)  $N_\gamma^{sd}$

Figure 6: Shakedown limit coefficients for a rolling point contact problem

391 When  $c$  is equal to zero, no resistance can be provided by the self-weight of the material (i.e.,  $N_c^{sd} = 0$   
 392 when  $\gamma a/c = \text{infinite}$ ), and the first term of Eq. 19 is also zero, so that the shakedown limit is zero for this  
 393 problem. This means, theoretically speaking, purely frictional soils will always fail if it is directly under a  
 394 repeated moving load.

395 It can also be deduced from Eq. 19 and Figure 6 that, for a certain soil, the size of the contact area only  
 396 affects the resistance from the self-weight of the soil. The influence of the enlarged contact area on the  
 397 shakedown capacity is competitively affected by increasing  $a$  and decreasing  $N_\gamma^{sd}$ . When  $a$  is very large,  
 398 its effect on  $N_\gamma^{sd}$  becomes very small; and therefore the shakedown limit tends to increase proportionally  
 399 with  $a$ . This also explains that the slab track problems have much larger shakedown limits compared to the  
 400 pavement problems. Apart from that, the overburden stress due to self-weight of superstructures in slab  
 401 tracks also contribute to the high shakedown limit.

402 It should be noted that, the theoretical shakedown limit will not be affected by the lateral earth pressure  
 403 coefficient  $k$ . Despite of that, the two critical residual stress fields (Eq. 5 and Eq. 6) at the shakedown limit  
 404 are changed by  $k$ , as shown in Figure 7. As explained in Yu and Wang (2012) and Wang and Yu (2013a),  
 405 when the applied load is at the shakedown limit, the actual residual stress field must lie within the region  
 406 bracketed by the two critical residual stress fields (i.e.  $\sigma_{xx-l}^r \leq \sigma_{xx}^r \leq \sigma_{xx-u}^r$ ); and the critical point is  
 407 located at the depth where the two fields just meet. It can be seen from Figure 7, the critical depth is not

408 changed by the lateral earth pressure coefficient  $k$ , but the residual stress at the critical depth (i.e. critical  
 409 residual stress) varies. A relatively small  $k$  value gives rise to a smaller (i.e. more compressive) critical  
 410 residual stress and therefore yields an identical shakedown solution. This indicates that soils always tend to  
 411 deform in a way that facilitate structural shakedown.

412

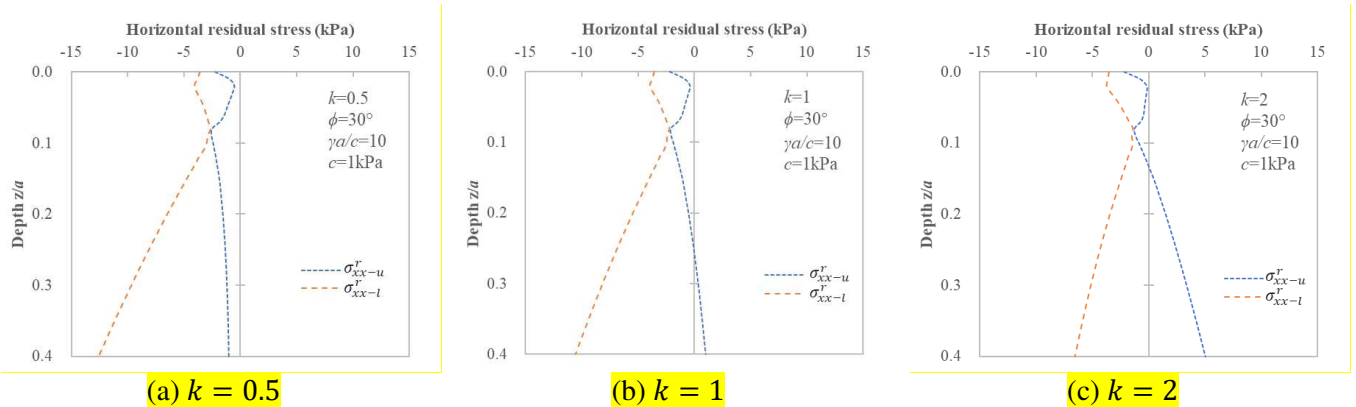


Figure 7: Distributions of critical residual stresses at shakedown limit  $q_{ult}^{sd} = 25.4 \text{ kPa}$

413

## 414 7 Concluding remarks

415 In this paper, a review of the recent development of the shakedown analysis methods for pavement and  
 416 railway applications was presented, including a brief recall of one static shakedown analysis based on  
 417 critical residual stress fields and one kinematical shakedown analysis using a nonlinear programming  
 418 approach. Comparison of the shakedown limits from different methods for a rolling and sliding point  
 419 contact problem showed generally good agreements. It was found that the shakedown limits of pavements  
 420 are mainly affected by the form of the contact loading, material properties, layer thicknesses, and  
 421 temperature. For railway problems, the influences of at-rest stress, subsoil stiffness variation, and velocity  
 422 factor could become significant.

423 A novel contribution of the paper is the introduction of a simple, unified equation for shakedown limit (or  
 424 cyclic capacity) of soils under repeated moving surface loads. This equation can be applied in a similar  
 425 manner to Terzaghi's bearing capacity equation, to provide different shakedown capacities for various

426 pavement or railway problems. Different from Terzaghi's equation, the coefficient  $N_{\gamma}^{sd}$  in the self-weight  
427 term depends on not only the soil friction angle but also the dimensionless factor  $\gamma a/c$ , and it is much  
428 smaller than the coefficient  $N_c^{sd}$  in the cohesion term. The influence of a rising contact area on the  
429 shakedown limit is competitively controlled by the increase of  $a$  and the decrease of  $N_{\gamma}^{sd}$ . The lateral earth  
430 pressure coefficient  $k$  does not influence the shakedown limit and the critical depth, but it changes the  
431 critical residual stress fields. Finally, this equation can be extended to consider other factors by  
432 incorporating correction coefficients, so that the shakedown or cyclic capacities for different pavement and  
433 railway problems can be determined.

434 It should be noted that the existing shakedown analyses were usually conducted by assuming that material  
435 strength parameters do not change with time or the number of loading cycles. Based on this assumption,  
436 the influence of various factors could be thoroughly investigated, that contributes to the selection of design  
437 alternatives. In reality, shakedown phenomena observed in pavements or railways should be attributed to  
438 two mechanisms: one is the structural shakedown due to the build-up of residual stresses in the structure  
439 without any change of its inner structure, which could be interpreted as the pure increase of contact forces  
440 among soil particles; the other is the change of the soil inner structure due to cyclic loads or time, which  
441 may advantage (e.g., densification of sand) or disadvantage (e.g., degradation of clay) the soil strength and  
442 thus increase or decrease the shakedown limit. This paper focused on the structural shakedown due to the  
443 first mechanism. The influence of the second mechanism needs to be further explored for different types of  
444 soils.

#### 445 **Reference list**

- 446 Bleich H., 1932. Über die Bemessung statisch unbestimmter Stahlwerke unter der Berücksichtigung der  
447 elastisch-plastischen Verhaltens des Baustoffes. Bauingenieur. 13, 261-269.
- 448 Boulbibane M., Collins I.F., Ponter A.R.S., Weichert D., 2005. Shakedown of unbound pavements. Road  
449 Mater Pavements Des. 6, 81-96.
- 450 Boulbibane M., Collins I.F., Weichert D., Raad L., 2000. Shakedown analysis of anisotropic asphalt  
451 concrete pavements with clay subgrade. Can Geotech J. 37, 882-889.
- 452 Boulbibane M., Ponter A.R.S., 2005. Extension of the linear matching method to geotechnical problems.  
453 Comput Methods Appl Mech Eng. 194, 4633-4650.

454 Boulbibane M., Ponter A.R.S., 2006. The linear matching method for the shakedown analysis of  
455 geotechnical problems. *Numer Analyt Meth Geomech.* 30, 157-179.

456 Boulbibane M., Weichert D., 1997. Application of shakedown theory to soils with non associated flow rules.  
457 *Mech Res Commun.* 24, 513-519.

458 Bower A.F., Johnson K.L., 1991. Plastic flow and shakedown of the rail surface in repeated wheel-rail  
459 contact. *Wear.* 144, 1-18.

460 Brown S.F., Juspi S., Yu H.S., 2008. Experimental observations and theoretical predictions of shakedown  
461 in soils under wheel loading, in: Ellis E., Yu, H.S., McDowell G., Dawson, A. and Thom, N. (Eds.),  
462 *Advances in Transportation Geotechnics*, pp. 707-712.

463 Brown S.F., Yu H.S., Juspi S., Wang J., 2012. Validation experiments for lower-bound shakedown theory  
464 applied to layered pavement systems. *Géotechnique.* 62, 923-932.

465 Ceradini G., 1969. Sull'adattamento dei corpi elastoplastici soggetti ad azioni dinamiche. *Giornale del*  
466 *Genio Civile.* 415, 239-258.

467 Ceradini G., 1980. Dynamic shakedown in elastic-plastic bodies. *J Engin Mech Div.* 106, 481-499.

468 Chazallon C., Allou F., Hornych P., Mouhoubi S., 2009. Finite elements modelling of the long-term  
469 behaviour of a full-scale flexible pavement with the shakedown theory. *Numer Analyt Meth Geomech.* 33,  
470 45-70.

471 Chen H.F., Ponter A.R.S., 2005. The linear matching method for shakedown and limit analysis applied to  
472 rolling and sliding point contact problems. *Road Mater Pavements Des.* 6, 9-30.

473 Collins I.F., Boulbibane M., 1998. The application of shakedown theory to pavement design. *Met Mater*  
474 *Int.* 4, 832-837.

475 Collins I.F., Boulbibane M., 2000. Geomechanical analysis of unbound pavements based on shakedown  
476 theory. *J Geotech Geoenviron.* 126, 50-59.

477 Collins I.F., Cliffe P.F., 1987. Shakedown in frictional materials under moving surface loads. *Numer Analyt*  
478 *Meth Geomech.* 11, 409-420.

479 Collins I.F., Wang A.P., Saunders L.R., 1993a. Shakedown in layered pavements under moving surface  
480 loads. *Numer Analyt Meth Geomech.* 17, 165-174.

481 Collins I.F., Wang A.P., Saunders L.R., 1993b. Shakedown theory and the design of unbound pavements.  
482 *Road Trans Res.* 2, 28-39.

483 Costa P.A., Lopes P., Cardoso A.S., 2018. Soil shakedown analysis of slab railway tracks: Numerical  
484 approach and parametric study. *Transp Geotech.* 16, 85-96.

485 Doyle N.F., 1980. *Railway track design: a review of current practices.* Australian Government Publisher  
486 Service, Canberra, Australia.

487 Dyson I.N., Williams J.A., Kapoor A., 1999. The effect of surface hardening on the elastic shakedown of  
488 elliptical contacts. *P I Mech Eng J: Eng Tribology.* 213, 287-298.

489 Hasan N., 2019. *Shakedown Limits and Uses in Railroad Engineering.* *J Mater Civ Eng.* 31,

490 Hills D.A., Sackfield A., 1984. Yield and shakedown states in the contact of generally curved bodies. *The*  
491 *Journal of Strain Analysis for Engineering Design.* 19, 9-14.

492 Juspi S., 2007. *Experimental validation of the shakedown concept for pavement analysis and design*, PhD  
493 thesis, University of Nottingham, UK.

494 Kapoor A., Williams J.A., 1994. Shakedown limits in sliding contacts on a surface-hardened half-space.  
495 *Wear.* 172, 197-206.

496 Koiter W.T., 1960. General theorems for elastic-plastic solids, in: Sneddon I.N., Hill R. (Eds.), *Progress of*  
497 *Solid Mechanics*, pp. 167-221.

498 König J.A., 1987. *Shakedown of elastic-plastic structures.* Elsevier Science Ltd., New York, US.

499 Krabbenhøft K., Lyamin A.V., Sloan S.W., 2007. Shakedown of a cohesive-frictional half-space subjected  
500 to rolling and sliding contact. *Int J Solids Struct.* 44, 3998-4008.

501 Lekarp F., Dawson A., 1998. Modelling permanent deformation behaviour of unbound granular materials.  
502 *Constr Build Mater.* 12, 9-18.



503 Li H.X., 2009. Kinematic shakedown analysis under a general yield condition with non-associated plastic  
504 flow. *Int J Mech Sci*.

505 Li H.X., Yu H.S., 2006. A nonlinear programming approach to kinematic shakedown analysis of frictional  
506 materials. *Int J Solids Struct*. 43, 6594-6614.

507 Liu S., Wang J., 2019. Application of shakedown theory in track substructure design. *P I Civil Eng: Ground*  
508 *Improv*. 172, 116-123.

509 Liu S., Wang J., Yu H.-S., Wanatowski D., 2016. Shakedown solutions for pavements with materials  
510 following associated and non-associated plastic flow rules. *Comput Geotech*. 78, 218-226.

511 Liu S., Wang J., Yu H.-S., Wanatowski D., 2018. Shakedown for slab track substructures with stiffness  
512 variation. *Geotech Res*. 5, 31-38.

513 Liu S., Wang J., Yu H.S., Wanatowski D., 2017. Numerical shakedown and non-shakedown responses of  
514 a Tresca half-space to a three-dimensional moving load, in: *Proceedings of 19th International Conference*  
515 *on Soil Mechanics and Geotechnical Engineering*, Seoul, Korea, 17-22 Sep 2017, pp. 1385-1388.

516 Liu S., Wang J., Yu H.S., Wanatowski D., Thom N., Grenfell J., 2020. Shakedown of asphalt pavements  
517 considering temperature effect. *International Journal of Pavement Engineering*. 1-12.

518 Maier G., 1969. Shakedown theory in perfect elastoplasticity with associated and nonassociated flow-laws  
519 - a finite element linear programming approach. *Meccanica*. 4, 250-260.

520 Melan E., 1938. Der Spannungszustand eines Henky-Mises schen Kontinuums bei Verlandicher Belastung.  
521 *Sitzungsberichte der Ak Wissenschaften Wien (Ser 2A)*. 147, 73.

522 Nguyen A.D., 2007. Lower-bound shakedown analysis of pavements by using the interior point method,  
523 PhD thesis, RWTH Aachen University, Aachen, Germany.

524 Nguyen A.D., Hachemi A., Weichert D., 2008. Application of the interior-point method to shakedown  
525 analysis of pavements. *Numer Analyt Meth Geomech*. 75, 414-439.

526 Ponter A.R.S., Carter K.F., 1997. Shakedown state simulation techniques based on linear elastic solutions.  
527 *Comput Methods Appl Mech Eng*. 140, 259-279.

528 Ponter A.R.S., Chen H.F., Ciavarella M., Specchia G., 2006. Shakedown analyses for rolling and sliding  
529 contact problems. *Int J Solids Struct*. 43, 4201-4219.

530 Ponter A.R.S., Engelhardt M., 2000. Shakedown limits for a general yield condition: Implementation and  
531 application for a von mises yield condition. *Eur J Mech A/Solids*. 19, 423-445.

532 Ponter A.R.S., Hearle A.D., Johnson K.L., 1985. Application of the kinematical shakedown theorem to  
533 rolling and sliding point contacts. *J Mech Phys Solids*. 33, 339-362,.

534 Prager W., 1948. Problem types in the theory of perfectly plastic materials. *J Aeronaut Sci*. 15, 337-341.

535 Pycko S., Maier G., 1995. Shakedown theorems for some classes of nonassociated hardening elastic-plastic  
536 material models. *Int J Plast*. 11, 367-395.

537 Qian J., Dai Y., Huang M., 2020. Dynamic shakedown analysis of two-layered pavement under rolling-  
538 sliding contact. *Soil Dyn Ear Eng*. 129, 105958.

539 Qian J., Lin H., Gu X., Xue J., 2018. Dynamic shakedown limits for flexible pavement with cross-  
540 anisotropic materials. *Road Mater Pavements Des*. 21, 310-330.

541 Qian J., Wang Y., Wang J., Huang M., 2017. The influence of traffic moving speed on shakedown limits  
542 of flexible pavements. *International Journal of Pavement Engineering*. 20, 233-244.

543 Qian J., Wang Y.G., Yin Z.Y., Huang M.S., 2016. Experimental identification of plastic shakedown  
544 behavior of saturated clay subjected to traffic loading with principal stress rotation. *Eng Geol*. 214, 29-42.

545 Raad L., Weichert D., 1995. Stability of pavement structures under long term repeated loading, in: Mroz Z.  
546 (Eds.), *Inelastic Behaviour of Structures under Variable Loads*, pp. 473-496.

547 Raad L., Weichert D., Haidar A., 1989a. Analysis of full-depth asphalt concrete pavements using  
548 shakedown theory. *Transp Res Board*. 1227, 53-65.

549 Raad L., Weichert D., Haidar A., 1989b. Shakedown and fatigue of pavements with granular bases. *Transp*  
550 *Res Board*. 1227, 159-172.

551 Raad L., Weichert D., Najm W., 1988. Stability of multilayer systems under repeated loads. *Transp Res*  
552 *Board*. 1207, 181-186.

553 Radovsky B.S., Murashina N.V., 1996. Shakedown of subgrade soil under repeated loading. *Transp Res*  
554 *Rec.* 82-88.

555 Rahmani R., Binesh S.M., 2018. Mesh-free shakedown analysis of cohesive-frictional pavement under  
556 moving traffic loads: deterministic and probabilistic frameworks. *Road Mater Pavements Des.* 1-39.

557 Ravindra P.S., 2008. Shakedown analysis of road pavements - an experimental point of view, PhD thesis,  
558 University of Sydney, Australia.

559 Ravindra P.S., Small J.C., 2008. Shakedown analysis of road pavements, in: *Proceedings of The 12th*  
560 *International Conference of International Association for Computer Methods and Advances in*  
561 *Geomechanics*, Goa, India, 1-6 Oct 2008, pp. 4432-4438.

562 Ringsberga J.W., F.J. F., B.L. J., A. K., J.C.O. N., 2005. Fatigue evaluation of surface coated railway rails  
563 using shakedown theory, finite element calculations, and lab and field trials. *Int J Fatigue.* 27, 680–694.

564 Sharp R.W., 1985. Pavement design based on shakedown analysis. *Transp Res Rec.* 1022, 107.

565 Sharp R.W., Booker J.R., 1984. Shakedown of pavements under moving surface loads. *J Transp Eng.* 110,  
566 1-14.

567 Shiau S.H., 2001. Numerical methods for shakedown analysis of pavements under moving surface loads,  
568 PhD thesis, University of Newcastle, Australia.

569 Shiau S.H., Yu H.S., 2000. Load and displacement prediction for shakedown analysis of layered pavements.  
570 *Transp Res Rec.* 1730, 117-124.

571 Tang L.S., Chen H.K., Sang H.T., Zhang S.Y., Zhang J.Y., 2015. Determination of traffic-load-influenced  
572 depths in clayey subsoil based on the shakedown concept. *Soil Dyn Ear Eng.* 77, 182–191.

573 Wang J., 2011. Shakedown analysis and design of flexible road pavements under moving surface loads,  
574 PhD thesis, University of Nottingham, UK.

575 Wang J., Liu S., Yang W., 2018a. Dynamics shakedown analysis of slab track substructures with reference  
576 to critical speed. *Soil Dyn Ear Eng.* 106, 1-13.

577 Wang J., Liu S., Yu H.S., 2016. A comparison between a shakedown design approach and the analytical  
578 design approach in the UK for flexible road pavements. *Procedia Eng.* 143, 971-978.

579 Wang J., Liu S., Yu H.S., 2018b. Recent progress on lower-bound shakedown analysis of road pavements,  
580 in: Barrera O., Cocks A., Ponter A. (Eds.), *Advances in Direct Methods for Materials and Structures*,  
581 Springer International Publishing, Cham, Switzerland, pp. 129-142.

582 Wang J., Xiong Y., Wanatowski D., 2020a. HCA study of permanent deformation of sand under train-  
583 induced stress path considering variable confining pressure, in: Tutumluer E., Chen X., Xiao Y. (Eds.),  
584 *Advances in Environmental Vibration and Transportation Geodynamics*, Springer, Singapore, pp. 347-357.

585 Wang J., Yu H.-S., Liu S., 2021. Shakedown limits of slab track substructures and their implications for  
586 design, in: Pisano A.A., Spiliopoulos K.V., Weichert D. (Eds.), *Direct Methods: Methodological Progress*  
587 *and Engineering Applications*, Springer, Cham, pp. 211-225.

588 Wang J., Yu H.S., 2013a. Residual stresses and shakedown in cohesive-frictional half-space under moving  
589 surface loads. *Geomech Geoengin.* 8, 1-14.

590 Wang J., Yu H.S., 2013b. Shakedown analysis for design of flexible pavements under moving loads. *Road*  
591 *Mater Pavements Des.* 14, 703-722.

592 Wang J., Yu H.S., 2014. Three-dimensional shakedown solutions for anisotropic cohesive-frictional  
593 materials under moving surface loads. *Numer Analyt Meth Geomech.* 38, 331-348.

594 Wang T., Luo Q., Liu J., Liu G., Xie H., 2020b. Method for slab track substructure design at a speed of  
595 400 km/h. *Transp Geotech.* 24,

596 Werkmeister S., Dawson A., Wellner F., 2001. Permanent deformation behavior of granular materials and  
597 the shakedown concept. *Transp Res Rec.* 1757, 75-81.

598 Xiao J.H., Wang B.L., Liu C.Y., Yu Z., 2016. Influences of subgrade form and ground stiffness on dynamic  
599 responses of railway subgrade under train loading: Field testing case study. *Procedia Eng.* 143, 1185-1192.

600 Xiao Y., Zheng K., Chen L., Mao J., 2018. Shakedown analysis of cyclic plastic deformation characteristics  
601 of unbound granular materials under moving wheel loads. *Constr Build Mater.* 167, 457-472.

602 Yu H.S., 2005. Three-dimensional analytical solutions for shakedown of cohesive-frictional materials under  
603 moving surface loads. *Proc R Soc A*. 461, 1951-1964.  
604 Yu H.S., Hossain M.Z., 1998. Lower bound shakedown analysis of layered pavements discontinuous stress  
605 fields. *Comput Methods Appl Mech Eng*. 167, 209-222.  
606 Yu H.S., Wang J., 2012. Three-dimensional shakedown solutions for cohesive-frictional materials under  
607 moving surface loads. *Int J Solids Struct*. 49, 3797–3807.  
608 Zhao J.D., Sloan S.W., Lyamin A.V., Krabbenhøft K., 2008. Bounds for shakedown of cohesive-frictional  
609 materials under moving surface loads. *Int J Solids Struct*. 45, 3290–3312.  
610 Zhuang Y., Wang K.Y., Li H.X., Wang M., Chen L., 2019. Application of three-dimensional shakedown  
611 solutions in railway structure under multiple Hertz loads. *Soil Dyn Ear Eng*. 117, 328-338.